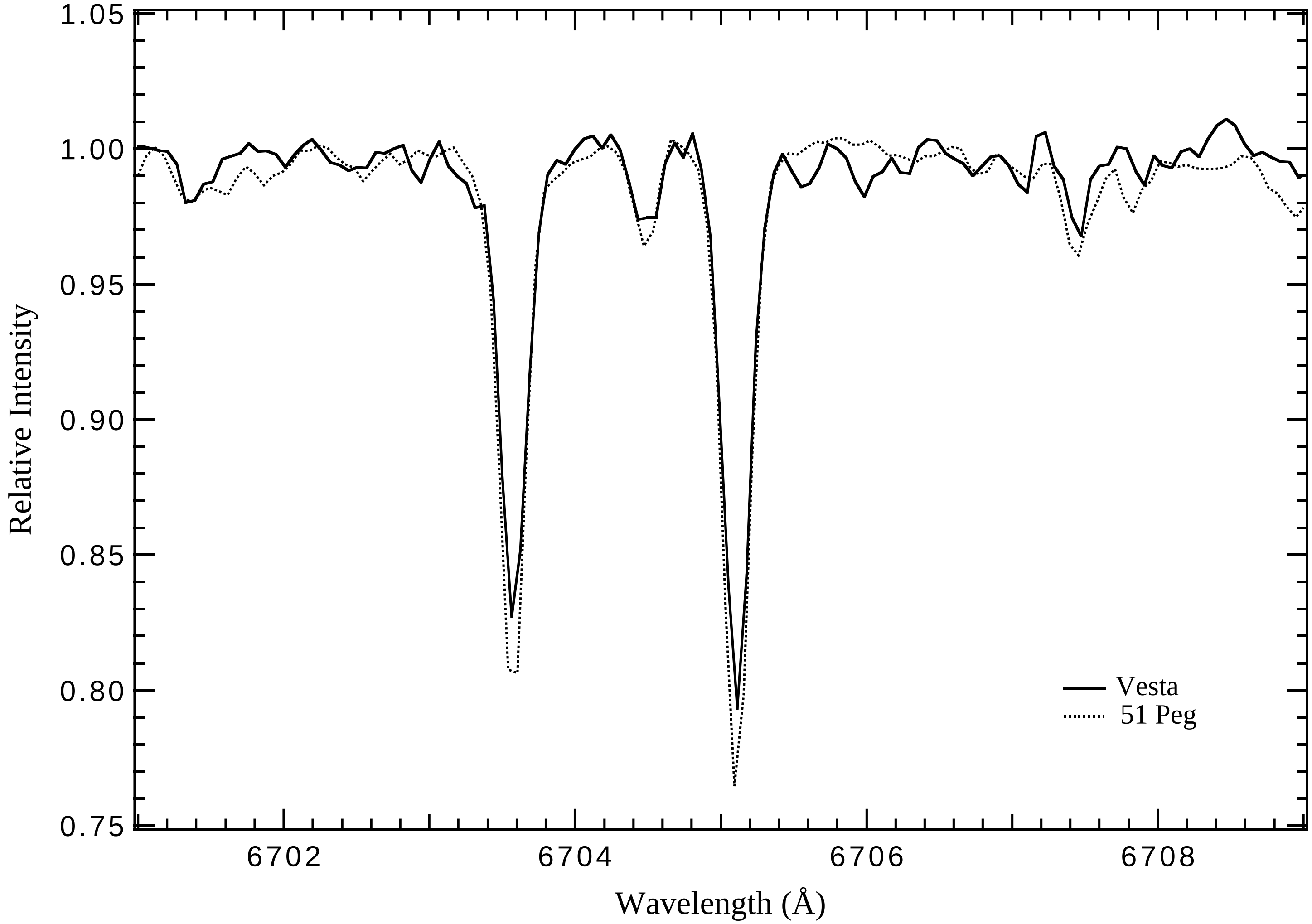

Relative Intensity
1.05
1.00
0.95
0.90
0.85
0.80
0.75
6702
6704
6706
6708
Wavelength (Å)
Vesta
51 Peg

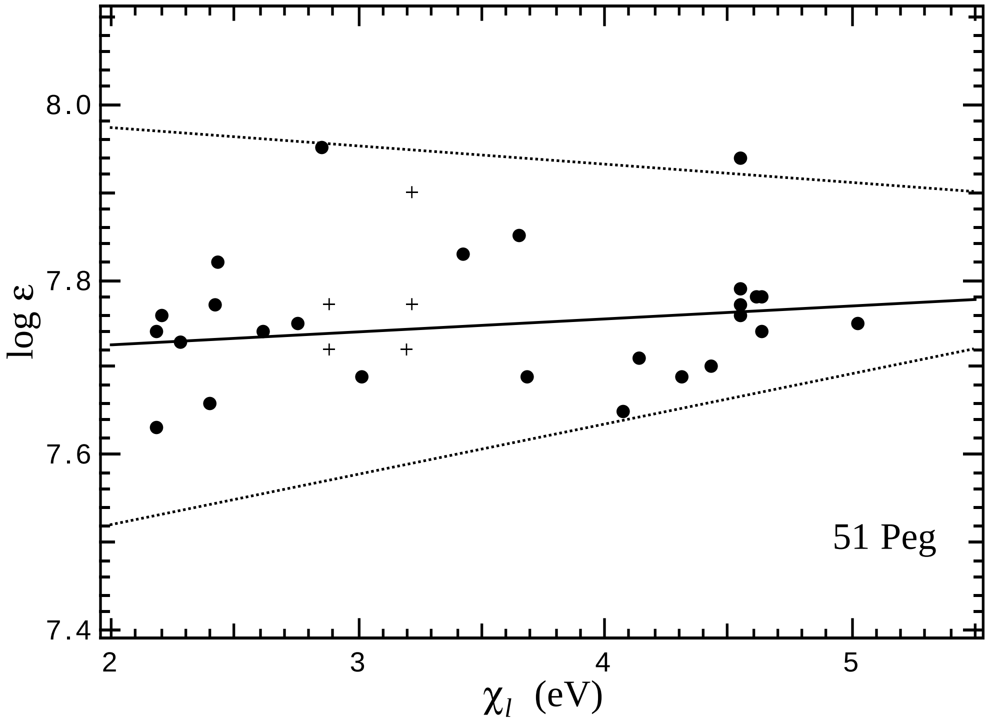
8.0
7.8
7.6
7.4
log ε
2
3
4
5
χ_l (eV)
51 Peg

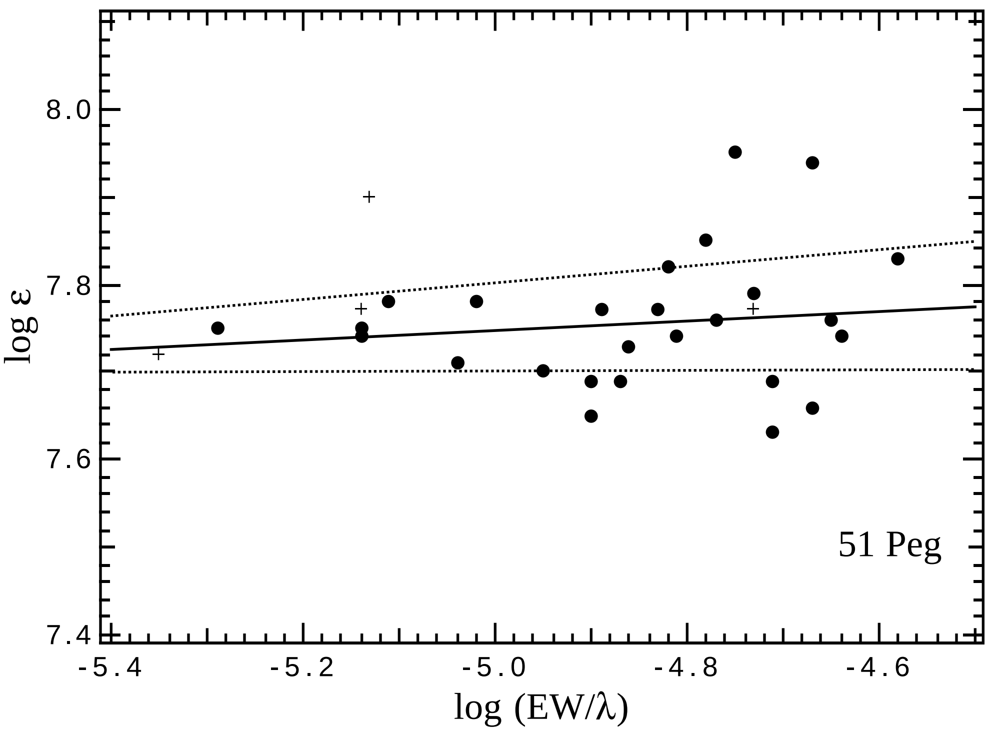
8.0
7.8
7.6
7.4
log ε
-5.4
-5.2
-5.0
-4.8
-4.6
log (EW/λ)
51 Peg

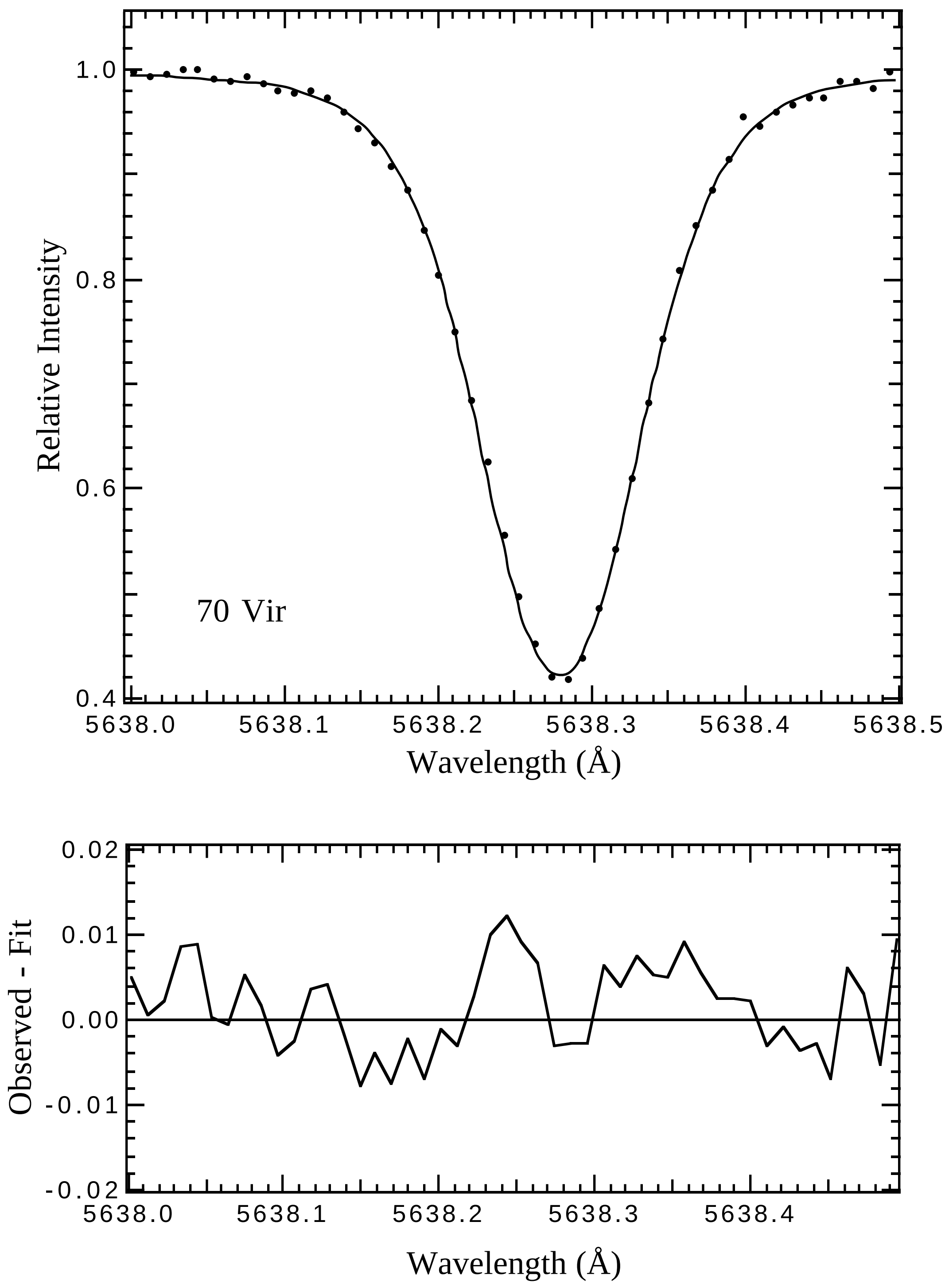

1.0
0.8
0.6
0.4
Relative Intensity
70 Vir
5638.0
5638.1
5638.2
5638.3
5638.4
5638.5
Wavelength (Å)
0.02
0.01
0.00
-0.01
-0.02
Observed - Fit
5638.0
5638.1
5638.2
5638.3
5638.4
Wavelength (Å)

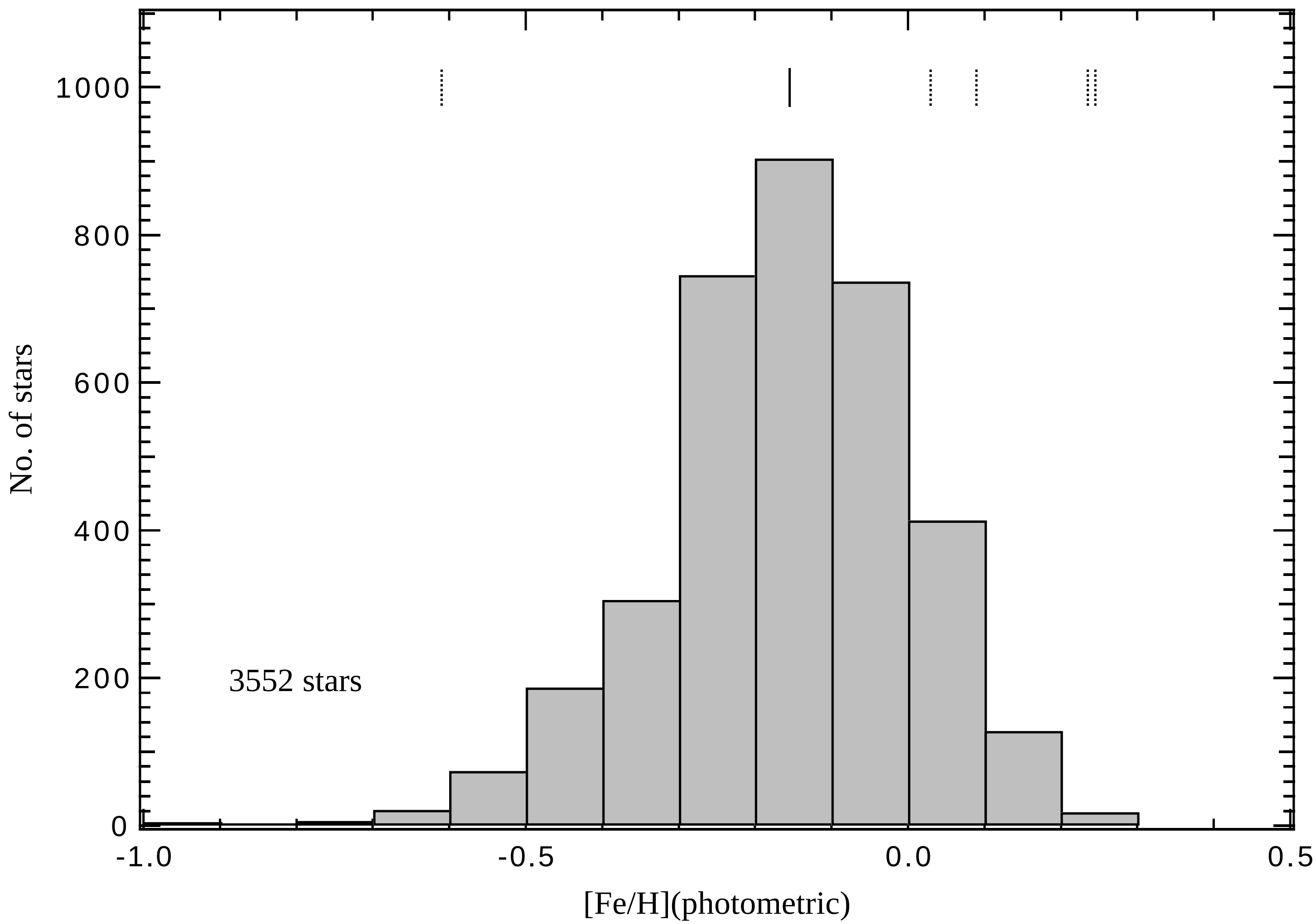

1000
800
600
400
200
0
No. of stars
3552 stars
-1.0
-0.5
0.0
0.5
[Fe/H](photometric)

Spectroscopic Ananlyses of the Planetary System Candidates: 55 Cnc, 51 Peg, 47 UMa, 70 Vir, and HD 114762

Guillermo Gonzalez

Department of Astronomy, University of Texas, Austin, TX 78712

Received ______________________; accepted ______________________

ABSTRACT

The stars 55 Cnc, 51 Peg, 47 UMa, 70 Vir, and HD 114762 have recently been proposed to harbor planetary mass companions. Using spectroscopic methods we find that 55 Cnc and 51 Peg are super metal-rich, 47 UMa and 70 Vir have roughly solar metallicities, and HD 114762 is metal-poor. Otherwise, the abundance patterns, expressed as [X/Fe], are approximately solar. The ages of 47 UMa and 51 Peg are similar to that of the Sun; 70 Vir is slightly older, and 55 Cnc and HD 114762 are at least 10 Gyrs old. Our estimates of $v \sin i$ for the parent stars are 1.4 ± 0.5, 1.8 ± 0.4, 2.0 ± 0.3, < 1, and < 1.5 km s^{-1} for 55 Cnc, 51 Peg, 47 UMa, 70 Vir, and HD 114762, respectively. Using these data and estimates for the rotation periods and radii, the corresponding masses of the companions are: > 0.6, $0.51^{+0.22}_{-0.03}$, 4.6 ± 1.0, > 20, and > 8.5 M_J. The systems appear to fall into three groups: roughly Jupiter mass companions with small circular orbits with metal-rich parent stars (55 Cnc and 51 Peg), larger companions with larger circular orbits (47 UMa), and much more massive companions with large eccentric orbits orbiting moderately metal-poor parent stars (70 Vir and HD 114762).

Our findings are consistent with a recently proposed mechanism whereby a gas giant migrates to within a few hundredths of an AU of its parent star during the formative epoch of the planetary system. During this process the material between the giant planet and the star is accreted onto the latter. If the accreted material is depleted in H and He, then the photospheric composition of the parent star might be altered significantly.

Subject headings: stars: abundances — stars: fundamental parameters — stars: planetary systems

1. Introduction

Between October 1995 and April 1996 the discovery of four candidate extra-solar systems (55 Cnc, 51 Peg, 47 UMa, and 70 Vir) were announced (Mayor & Queloz 1995; Butler & Marcy 1996; Marcy & Butler 1996a); another candidate, HD 114762, was discovered by Latham et al. (1989) . These historic discoveries are the fruits of about 15 years of searching by several groups (Campbell et al. 1988; Cochran & Hatzes 1995; Walker et al. 1995), most of which have not yet found independent evidence of planetary mass companions. Now, theoreticians have empirical data to test their planet formation models. One aspect of planet formation that has not been discussed in much detail is the dependence of planet formation on the metallicity of the protostellar cloud. With five planetary system candidates (and one certain case, the Solar System), we can begin to address this question.

The primary purpose of this study is to accurately determine the metallicities of the photospheres of 55 Cnc, 51 Peg, 47 UMa, 70 Vir, and HD 114762. We also attempt to estimate the abundances of about 15 other elements including lithium, which can to used to constrain their ages. While others have performed abundance analyses on these stars already, we analyze them together as a homogenous group; our analysis also serves as a check of previous studies. As a secondary goal, we also derive accurate estimates of $v \sin i$ for these stars, and, combining them with other data, use them to place constraints on the masses of the companions.

2. Observations

Moderate resolution spectra ($R \approx 60000$) were obtained by the author on five observing runs of two to three nights each between December 1995 and May 1996 at the McDonald observatory using the 2.1 m telescope equipped with a Cassegrain echelle and a 1200 x 400

pixel Reticon detector (McCarthy et al. 1993). Each star was observed no more than once per night with exposure times typically between one and five minutes, resulting in spectra with S/N ratios between 150 and 300. These spectra will be used in §3.1 for the purpose of deriving abundance estimates for the program stars.

For the purpose of studying line profile shapes, additional spectra were obtained at the author's request by David L. Lambert and Eric Bakker using the 2.7 m telescope equipped with the 2dcoudé echelle giving spectral resolutions (depending on the slit width) near 230000 for 47 UMa, 70 Vir, and HD 114762, 115000 for 51 Peg, and 180000 for 55 Cnc (instrument described by Tull et al. 1995); the S/N ratios are in the range of 250 to 350, except for HD 114762, which is near 200. The (incomplete) spectral coverage is 4700 - 5800 Å for 47 UMa, 70 Vir and HD 114762 and 5700 - 7900 Å for 51 Peg. Each observation was broken up into two or three exposures in order to detect and eliminate cosmic ray hits on the images. The procedures followed in reducing the spectra are described in Gonzalez & Lambert (1996). A sample spectrum of 51 Peg overplotted with the solar spectrum is shown in Figure 1.

3. Analysis

3.1. Abundance Analysis

Our method of abundance analysis closely follows that used by Gonzalez & Lambert in their study of several stars in the α Per cluster. Consequently, this analysis is a differential one with respect to the Sun. Since the stars on our program are similar to the Sun in their physical characteristics, a differential abundance analysis with the Sun as the source of the gf-values avoids many possible systematic errors. Two of these include uncertainties in the treatment of the structure of the atmospheres, such as differences in the mixing length to

scale height ratio or convection and differences in the area covered by sunspots [1]. Following Gonzalez & Lambert we employ the Kurucz (1992) model atmospheres; the effective temperature, $T_{\rm eff}$, surface gravity, g, and depth-independent microturbulence parameter, $\xi_{\rm t}$, are estimated in the standard way using the Fe I and Fe II lines (details are discussed in the next section).

The abundance analyses of 55 Cnc, 51 Peg, 47 UMa, 70 Vir, and HD 114762 are based on measurements of the moderate resolution spectra obtained with the 2.1 m telescope. The linelist used in the present analysis was selected from the lines published in Tables 12 and 13 by Gonzalez & Lambert. Additional lines were added (Table 1) and their gf-values estimated using the equivalent widths (EW's) measured on the Solar Flux Atlas (Kurucz et al. 1984). Although the wavelength coverage is quite extensive and the quality of the spectra is high, we have been very restrictive in our selection of lines. To be suitable, a line must be unblended (except for a few rare cases when the line is critical to estimating the abundance of a given element) and have a symmetric profile in both the target star spectrum and the solar spectrum. The sample is restricted to mostly moderate strength lines between about 20 and 150 mÅ. Weaker lines have a larger relative error in the EW estimates due to noise, and stronger lines are more sensitive to errors in $\xi_{\rm t}$; based on measurements of the same lines on spectra taken on different nights, we estimate that the average uncertainty in an EW estimate to be about ± 1-2 mÅ for lines with EW = 20 - 60 mÅ and about ± 2-3 mÅ for stronger lines. Such low errors were achieved by smoothing isolated lines (effectively increasing the S/N ratio), measuring some lines on the overlap regions of adjacent orders, and averaging EW measurements obtained on different observing

---

[1]The sunposts may vary on a monthly or yearly basis. Also, the area covered by sunspots averaged over a sunspot cycle may vary from star to star; this may not be a problem for solar type stars younger than the Sun typically display stronger chromospheric activity.

runs. The range in measured line strengths is sufficient to estimate ξ_t accurately. The Fe I lines employed in the analysis have lower excitation potentials,χ_l, ranging from 2.2 to 5.0 eV; this is sufficient to estimate $T_{\rm eff}$ accurately for each of the program stars.

3.1.1. Model Atmosphere Selection and Fe Abundances

While hundreds of Fe lines are present in the spectral regions observed, we selected only 26 Fe I and 5 Fe II for use in the analysis (the total number varies from star to star). The values of $T_{\rm eff}$, $\log g$, and ξ_t have been estimated with this sample of Fe lines (Table 2). The typical uncertainties in these parameters are ± 100 K, ± 0.1 (cgs), and ± 0.1 km s^{-1}, respectively; the individual uncertainties are listed in Table 2. They lead to a typical uncertainty in [Fe/H] of ± 0.07 dex, which was calculated using the sensitivities of the abundances to changes in atmospheric parameters (Table 3). The sensitivities of the $\log \epsilon_{\rm Fe}$ versus χ_l and $\log \epsilon_{\rm Fe}$ versus $\log (EW/\lambda)$ relationships to changes in $T_{\rm eff}$ and ξ_t, respectively, are shown in Figure 2 for 51 Peg. The measured EW's are listed in Table 4.

How do our estimates of [Fe/H] and $T_{\rm eff}$ compare to published estimates? They can be calculated from Strömgren $uvby - \beta$ narrow band photometry; such data exist for all the program stars (Hauck & Mermilliod 1990) [2]. Using the calibration equation between [Me/H] and the β and dm1 indices given by Nissen (1988), we estimate that [Me/H] is 0.27, 0.03, -0.06, and -0.79 for 51 Peg, 47 UMa, 70 Vir, and HD 114762, respectively (these photometric calibrations do not apply to 55 Cnc as it is too cool); Nissen claims

[2]The quantity [Me/H] refers to the logarithmic abundance of a metal relative to the sun. Technically, one actually measures [Me/H] with photometry rather than [Fe/H], since the spectral regions covered by the different Strömgren filters includes other elements in addition to iron.

his equation is accurate to within about ± 0.10 dex. Thus, given the uncertainties of our spectroscopic estimates, these photometric estimates are consistent with ours. Saxner & Hammarbäck (1985) derived equations relating the $b-y$ and β indices to $T_{\rm eff}$. While their calibrations are accurate to with about ± 60 K, we can improve upon them slightly by updating the photometry (using the mean values tabulated by Hauck & Mermilliod 1990) of the calibrating stars and restricting the sample to sharp- lined stars. With a sample of 16 stars, we derive,

$$T_{\rm eff} = 8178 - 5980(b-y)\{1 - 0.070[Fe/H]\} \tag{1}$$
$$T_{\rm eff} = 11495\sqrt{(\beta - 2.3405)}$$

The mean scatter in the first and second equations are ± 40 and ± 50 K, respectively. We list in Table 5 the resultant estimates of $T_{\rm eff}$ for each of our program stars using equation 1 and the mean Strömgren indices from Hauck & Mermilliod. Also listed in the table are the mean values of $T_{\rm eff}$ for each program star combining the photometric and spectroscopic estimates and the resultant corrected values of log g and [Fe/H] for each star. These new atmospheric parameters will be used in §4.2 to estimate the ages of the program stars.

3.1.2. Other Elements

The abundances of 15 additional elements were estimated using the atmospheric parameters given in Table 2. The individual line measurements are listed in Table 4. The uncertainties in the [X/H] values were calculated using the estimated uncertainties in the atmospheric parameters (Table 2) and the data in Table 3.

Since the resonance line of lithium is blended with other lines in spectra of solar-type stars, we must employ spectrum synthesis methods to estimate its abundance. We employed

the linelist given by Cunha et al. (1995, Table 7), modified slightly to reproduce the solar spectrum using the Kurucz solar model atmosphere (Kurucz 1992); the spectral region synthesized spans 6700 to 6710 ÅṪhe same stellar atmospheric parameters derived from the Fe-line analysis were used in producing the synthetic spectra. The line broadening was approximated with a Gaussian function in the synthetic spectra with a width chosen so that the two strong Fe I lines in the observed spectra are reproduced accurately. The lithium line is discernible by eye on all spectra, except that of 55 Cnc, where it is not detectable at the level of the noise. The final adopted lithium abundances for the three stars are listed in Table 6 along with the other elements.

3.2. $v \sin i$

In order to estimate the mass of a companion, we require, among other quantities, an estimate of the orbital inclination. Assuming the orbital axis is aligned with the stellar rotation axis, an estimate of the projected stellar equatorial rotational velocity ($v \sin i$) can be used to constrain the orbital inclination. In this section we describe the derivation of $v \sin i$ for the program stars from the high resolution spectra obtained with the 2.7 m telescope. In addition to the program star spectra, a spectrum of the sky was obtained in order to calibrate our technique with the known solar parameters.

Of the two methods most often used to estimate $v \sin i$ from a stellar spectrum, Fourier transform and profile synthesis, we opted for the latter. The instrumental, macroturbulent ($\zeta_{\rm RT}$), microturbulent ($\xi_{\rm t}$), rotational, and thermal broadening mechanisms are included in the analysis of the line profiles. The syntheses have been carried out with MOOG, modified to include macroturbulent line broadening in addition to the other line broadening mechanisms already present in the program. We have adopted the radial-tangential description of macroturbulent line broadening (Gray 1992) using the mathematical

formalism of Durrant (1979). The instrumental broadening is approximated by a Gaussian function, its width determined from the Th-Ar comparison spectrum obtained immediately following each stellar observation. This approximation is a very close fit to the Th-Ar lines; however, even if it were not, that would not cause significant errors since the instrumental broadening is relatively small compared to the other line broadeners. The limb darkening coefficients, required for synthesizing the rotational profiles, are interpolated from Figure 17.6 of Gray (1992). The model atmospheric parameters used in the syntheses are the same as those estimated from the Fe-line analyses in §3.1.1, except for $\xi_{\rm t}$. In their studies of the solar spectrum Gray (1977) and Takeda (1995) found that one must assume $\xi_{\rm t} = 0.5$ km s^{-1} in order to accurately reproduce the line profiles accurately.

The Fe I lines at 5379.586 and 5638.249 Å were selected for analysis from Table 2 of Takeda; these lines are unblended, are moderate in strength, and have smaller than average $\zeta_{\rm RT}$ values. This last criterion is particularly important in deriving accurate values of $v \sin i$, since $\zeta_{\rm RT}$ is the dominant broadening mechanism in our sample stars. The solar Fe I lines were analyzed first with $v \sin i$ held fixed at 1.9 km s^{-1} in order to estimate $\xi_{\rm t}$ and $\zeta_{\rm RT}$. The parameters were adjusted manually and the final parameters chosen when the residuals between the observed and synthetic line profiles were minimized. The value of $\xi_{\rm t}$ required to reproduce the line profiles is 0.4 km s^{-1}; our estimates of $\zeta_{\rm RT}$ are similar to those quoted by Takeda for the same lines. Treating $v \sin i$ as an additional free parameter leads to a very similar solution (Table 7). The apparent discrepancy in $\xi_{\rm t}$ obtained from the abundance analysis as compared to the line profile analysis has been noted by other researchers. However, it is only a scientific problem, not a practical one. The discrepancy is likely caused by model- incompleteness (cf. Takeda et al. 1996 for a brief discussion of this problem).

The values of $v \sin i$ for the other program stars were estimated for the program

stars in the same way as for the Sun. Zeeman broadening was not included in any of the analyses, since it is not found to be a significant source of line broadening for stars hotter that G6 (Gray 1984). This may not be the case for 55 Cnc, but as we show in §4.2, its low chromospheric activity implies that Zeeman broadening may not be significant for this star. The values of $v \sin i$ and $\zeta_{\rm RT}$ for the program stars were estimated assuming $\xi_{\rm t} = 0.4$ km s^{-1}, except for 47 UMa, where $\xi_{\rm t} = 0.45$ km s^{-1} was assumed. The estimated values for each spectral line are given in Table 7. The uncertainties quoted were estimated in a formal way by noting the change in residuals as the broadening parameters are changed. Taking into consideration Soderblom's (1982) conclusion that small $v \sin i$ estimates, those less than about 2 km s^{-1}, should be regarded as upper limits, we adopt the following values of $v \sin i$: 1.4 ± 0.5, 1.8 ± 0.4, 2.0 ± 0.3, < 1, and < 1.5 km s^{-1} for 55 Cnc, 51 Peg, 47 UMa, 70 Vir, and HD 114762, respectively. Slight asymmetries were detectable in some of the lines, but they did not affect the final solutions. A sample line profile fit is shown in Figure 3.

Previous estimates of $v \sin i$ exist for 51 Peg and HD 114762. The values of $v \sin i$ or 51 Peg are 2.1 ± 0.6 (Baranne et al. 1979), 1.7 ± 0.8 (Soderblom 1983), 2.8 ± 0.5 (Mayor & Queloz 1995), and 2.4 ± 0.3 km s^{-1} (François et al. 1996). Cochran et al. (1991) derived $v \sin i = 0^{+1}_{-0}$ km s^{-1} for HD 114762 assuming $\xi_{\rm t} = 1.0$ km s^{-1}, while Hale (1995) found $v \sin i = 0.8 \pm 0.7$ km s^{-1} assuming $\xi_{\rm t} = 0.7$ km s^{-1}.

4. Discussion

4.1. Abundances

All our program stars are listed in the catalog of Cayrel de Strobel et al. (1992), who compile spectroscopic [Fe/H] determinations from the literature. They list five estimates for HD 114762 averaging to -0.77, which is 0.16 dex less than our estimate. For the other

stars all the estimates are from the 1970's: there are four for 55 Cnc averaging to +0.13; 51 Peg, 47 UMa, and 70 Vir each have single estimates of +0.12, -0.02, and -0.11, respectively. Mayor & Queloz (1995) quote a recent (previously unpublished) spectroscopic estimate of [Fe/H] for 51 Peg of 0.19 dex and a Geneva photometric estimate of [Me/H] of 0.20 dex. Edvardsson et al. (1993) included 51 Peg, 47 UMa, and HD 114762 in their large survey of 189 nearby F and G dwarfs obtaining [Fe/H] values of +0.06, +0.01, and -0.74, respectively; these estimates are systematically smaller than ours by about 0.13 dex.

The photometric metallicity estimates of Edvardsson et al. are systematically higher than their spectroscopic estimates for the most metal-rich stars in their sample. Nissen (1994) addressed this discrepancy and claims that the problem is with the photometric metallicity calibration used by Edvardsson et al. In order to check the possibility that the different [Fe/H] estimates for 51 Peg are due to differences in the EW measurements, we have compared the Edvardsson et al. measurements (not included in their published paper; provided to the author by Bengt Edvardsson) to those of this study. The EW measurements of Edvardsson et al. are systematically smaller by about 15%; this is sufficient to account for the different [Fe/H] estimates of our studies. Our measurements, however, are very similar to those obtained recently by Jocelyn Tomkin, who has recently observed 51 Peg with the 2.7 m telescope at McDonald Observatory with a spectral resolution ≈ 60000. The spectral resolution used in the Edvardsson et al. (1993) study was only ≈ 30000. Such a low resolution, especially for a metal-rich star, might result in blending of the numerous weak lines, leading to the formation of a pseudo-continuum and apparent weakening of the stronger lines.

In his study of super metal-rich (SMR; defined as having [Fe/H] > 0.2) stars Taylor (1996; his Table 4) lists 29 SMR luminosity class IV-V candidates; 55 Cnc and 51 Peg are included in this list. Photometric estimates of [Fe/H] are +0.5 and +0.25 for 55 Cnc and

51 Peg, respectively; mean spectroscopic [Fe/H] values, based on published estimates and transformed to a uniform temperature and metallicity scale by Taylor, are 0.41 ± 0.10 and 0.17 ± 0.05, respectively. While having two of our program stars appear in a list of 29 suspected SMR stars seems significant, it becomes less so when one realizes that 10 of the nearly 120 stars analyzed by Marcy and Butler also appear on the list. More significant is the fact that 55 Cnc is one of the 7 stars with a probability *ge* 95% of being a SMR star; none of the other stars observed by Marcy & Butler is a member of this "magnificent seven." Including the results of our study and those of Mayor & Queloz (1995) leads us to conclude that 51 Peg is marginally also a SMR star.

As an illustration of the unusual metallicity distribution of our program stars, we compare them to the distribution of [Fe/H] values for nearby F and G dwarfs. Marsakov & Shevelev (1995) have estimated the [Fe/H] distribution from *uvby* photometry for 5489 F to early G dwarfs within 80 parsecs of the Sun. Their method involves using the $b - y$ color index as the independent variable in estimating [Fe/H], which is slightly less precise than the traditional method using the Strömgren β index as the independent variable. We have edited their dataset by removing unresolved binaries and stars with $T_{\rm eff} > 6500$ K, leaving 3552 stars in the sample (Figure 4). The mean value of [Fe/H] for this distribution is -0.16 dex. This result is similar to that of the more careful analysis of a smaller set of nearby dwarfs by Rocha-Pinto & Maciel (1996). As we will show below, the companions to 70 Vir and HD 114762 are not likely to be planetary in nature. This leaves 55 Cnc, 51 Peg, and 47 UMa as the best candidates harboring planets, which also happen to be the most metal-rich stars in our sample.

We do not confirm the finding of Edvardsson et al. (1993) that 51 Peg is a "NaMgAl" star. Apart from the general enhancements of the metals, the abundance patterns of the program stars are very similar to that of the Sun. To the best of our knowledge, the Li

abundance has only been estimated for one of our sample stars, 51 Peg; François et al. (1996) find that it has a solar Li abundance. The relevance of knowledge of the lithium abundances will be discussed in the next section.

4.2. Ages, Rotation Periods, and Masses

The $v \sin i$ estimates, when combined with the rotational velocities and mass estimates of the program stars, can be used to set limits on the masses of their companions. Given that angular velocity correlates fairly well with age for G dwarfs (Dorren et al. 1994; Soderblom 1985), age can be used to place useful constraints on the rotation periods for our sample. In this section we will estimate the ages, rotation velocities, and masses of the program stars as well as the masses of the companions using the atmospheric parameters derived in §3 and published data.

The most commonly used method of estimating the mass and age of a single main sequence or subgiant star involves comparing its observed physical parameters ($T_{\rm eff}$, $M_{\rm V}$, [Fe/H]) to theoretical stellar evolutionary sequences. We make use of the VandenBerg (1985) evolutionary stellar grids, extrapolated slightly to the metallicities of the program stars (VandenBerg did not calculate tracks above solar metallicity), to estimate their ages and masses. We first checked the accuracy of VandenBerg's calculations with the Sun. The theoretical tracks predict the correct value of $T_{\rm eff}$ for the Sun given its mass, age, and metallicity, but the theoretical value of and $M_{\rm V}$ must be reduced by 0.21 dex. We have derived two estimates of $M_{\rm V}$ for each star: one uses the HIPPARCOS parallax estimates of Perryman et al. (1996), except for 55 Cnc, which is from van Altena et al. (1995) corrected according to Lutz & Kelker (1973), the other uses the Strmgren photometric indices and equations 10 and 12 of Nissen (1988). The $M_{\rm V}$ estimates from the HIPPARCOS data are much more accurate; they were adopted instead of the photometric estimates

when available. We list the ages in Table 8, which were calculated using the atmospheric parameters given in Table 5 and the adopted $M_{\rm V}$ estimates, corrected using the factor derived from the solar case above. We can check the accuracy of our method with a star of known age; β Hyi is probably the best choice as it is the closest subgiant and has nearly the same temperature as the Sun. Using the physical stellar parameters of β Hyi given in Dravins et al. (1993), we derive an age of 12.5 $\pm$ 2.5 Gyr and a mass of 0.94 $\pm$ 0.04 $M_{\odot}$. Dravins et al. derived an age of 9.5 $\pm$ 0.8 Gyr and a mass of 0.99 $M_{\odot}$, consistent with our estimates. Edvardsson et al. (1993) derived age estimates for 51 Peg, 47 UMa, and HD 114762 also using the VandenBerg tracks; given the uncertainties, their results are generally in agreement with ours except for 51 Peg. This is not unexpected given our use of a more accurate estimate for $M_{\rm V}$ for this star.

There are other, less precise, age indicators that can be used to further constrain the ages of the stars. Several indicators have to do with the Galactic orbit. As a star ages, chance encounters with molecular clouds perturb it away from a simple circular orbit in the plane of the disk. Hence, both the maximum height reached above the Galactic plane, $Z_{\rm max}$, and the eccentricity,e, of its orbit generally increase with time. Among our sample, HD 114762 has the largest values of e and $Z_{\rm max}$, 0.27 and 0.90 kpc, respectively. Given the large scatter in the $Z_{\rm max}$ - age and e - age relations (see Edvardsson et al. 1993), we cannot say much more about the other stars, except that 47 UMa is likely the youngest. The total space velocity is another age indicator; the magnitudes of the space velocities for 55 Cnc, 51 Peg, 47 UMa, 70 Vir, and HD 114762 are 42.1, 38.0, 24.2, 26.9, and 104.8 km s^{-1}, respectively. Using the young-disk versus old-disk classification scheme of Eggen (1969; his Figure 1) based on U and V velocities, only HD 114762 clearly stands out as a member of the old-disk. Better age indicators are those related to the level of chromospheric activity. As a star ages, its chromospheric activity is seen to decline (Soderblom 1985; Dorren et al. 1994). Of our sample, all but HD 114762 were included in Soderblom's study of Ca II

emission strengths in solar-type dwarfs; of the remaining four stars, 47 UMa is found to be the youngest and 55 Cnc the oldest. Related to the level of chromospheric activity is the amplitude of the visual brightness; by the time a solar-type dwarf is about 3 Gyr old, the brightness variations drop below about 0.01 magnitudes (Dorren et al. 1994). Shortly after the discovery of 51 Peg B was announced in October 1995, 51 Peg was monitored photometrically and was found to be constant at the 0.0018 mag. level (Guinan 1995), implying that 51 Peg is at least a few billion years old. Finally, the lithium abundance might be used to constrain stellar age. This is more tricky, though, since the decline of lithium in a star's photosphere as it ages is followed eventually by a dramatic resurgence as the star ascends the subgiant branch (Dravins et al. 1993); it is somewhat variable from cluster to cluster. While there has been some progress in deriving the relation between age and lithium abundance for dwarfs (Soderblom et al. 1990), more recent work has shown that the relation is not be simple one (Lambert et al. 1991; Favata et al. 1996). Hence, while a large lithium abundance cannot tell us much by itself, a very low abundance is consistent with an intermediate age (neither very young on the ZAMS nor very old on its way up the subgiant branch). Using this criterion combined with our surface gravity estimates, it appears that HD 114762 is very old followed by 70 Vir and 55 Cnc. Combining all these secondary age criteria, the ages of the program stars, in descending order, are HD 114762, 70 Vir, 55 Cnc, 51 Peg, and 47 UMa. This order is similar, but not identical, to the order derived from the stellar evolutionary tracks.

The masses derived from the VandenBerg tracks are given in Table 10; the stellar radii, based on our estimates of $M_{\rm V}$ and $T_{\rm eff}$, are 1.03 ± 0.08, 1.14 ± 0.06, 1.20 ± 0.06, 1.83 ± 0.10, and 1.06 ± 0.21 $R_\odot$ for 55 Cnc, 51 Peg, 47 UMa, 70 Vir, and HD 114762, respectively. The uncertainties associated with the mass estimates may seem small, but for stars at or near the turnoff (such as 55 Cnc, 70 Vir, and HD 114762), the age and mass estimates are well-constrained by the observations; also, the mass and age estimates are well constrained

with the new HIPPARCOS data. Using Soderblom's (1985) estimates of angular rotation velocities, which he derived from $R_{\rm HK}$, the ratio of the mean Ca II H and K flux to the stellar bolometric flux, and an $R_{\rm HK}$ - angular velocity relation, we derive rotation periods of 44 $\pm$ 2, 29 $\pm$ 1, 16 $\pm$ 1, and 36 $\pm$ 2 days for 55 Cnc, 51 Peg, 47 UMa, and 70 Vir, respectively. Using Soderblom's equation 2 with his angular velocity estimates, the ages of the stars are 5.6 $\pm$ 0.6, 7.6 $\pm$ 1.7, 1.4 $\pm$ 0.4, and 18 $\pm$ 6 Gyr, respectively. These estimates are not in agreement with the ages derived earlier from the theoretical evolutionary tracks, which is not surprising given the indirect nature of the angular velocity - age relation. The rotation period has not been measured for HD 114762, but we will adopt a value of 45 $\pm$ 5 days based on its age. Baliunas et al. (1996), using Ca II H and K flux modulation observations, directly measured the rotation period of 51 Peg to be 37 days (they did not quote error bars). This apparent discrepancy between the Baliunas et al. and Soderblom rotation period estimates will need to be resolved in the future, but for now we will adopt 35 $\pm$ 2 days as the rotation period of 51 Peg.

Using the adopted values of $v \sin i$, rotation period, and radius for each star, we estimate the following values of $\sin i$: 1.18 $\pm$ 0.44, 1.09 $\pm$ 0.26, 0.53 $\pm$ 0.09, $<$ 0.39, and $<$ 1.26, for 55 Cnc, 51 Peg, 47 UMa, 70 Vir, and HD 114762, respectively. Obviously, values of $\sin i > 1.0$ are not acceptable; taking this into account, the new estimates become: $1.00^{+0.00}_{-0.28}$, $1.00^{+0.00}_{-0.17}$, 0.53 $\pm$ 0.09, $<$ 0.39, and $<$ 1.00. One additional source of uncertainty needs to be included in the $\sin i$ estimates - the degree of alignment between the orbital axis of the companion and rotational axis of the parent star, which we will represent as $i_{\rm orb} - i_{\rm rot} = \delta i$. Hale (1994) estimated that δi for solar-type binaries with semimajor axes less that 15 AU is about 10 degrees. Perhaps more relevant to the present analysis is the fact that the value of δi for Jupiter is only about 6 degrees. Including the additional uncertainty in the orbital inclination of $\pm$ 8 degrees, the values of $\sin i$ of the companions' orbits become $1.00^{+0.00}_{-0.38}$, $1.00^{+0.00}_{-0.26}$, $0.53^{+0.11}_{-0.12}$, $<$ 0.39, and $<$ 1.00.

Mayor & Queloz (1995) quote a mass function of (0.91 $\pm$ 0.15) x 10^{-10} $M_\odot$ for 51 Peg; Butler & Marcy (1996) and Marcy & Butler (1996a) quote (1.07 $\pm$ 0.23) x 10^{-8} and (2.98 $\pm$ 0.20) x 10^{-7} $M_\odot$ for 47 UMa and 70 Vir, respectively. Marcy & Butler (1996b) quote M$\sin i$ = 7.6 x 10^{-4} $M_\odot$ for 55 Cnc B (no error bars given). Cochran et al. (1991) determine a mass function of (1.6 $\pm$ 0.1) x 10^{-7} $M_\odot$ for HD 114762. Using these data and the values of $v \sin i$ quoted above we estimate the masses of the companions to be > 0.6, $0.51^{+0.22}_{-0.03}$, 4.6 $\pm$ 1.0, > 20, and > 8.5 M_J for 55 Cnc, 51 Peg, 47 UMa, 70 Vir, and HD 114762, respectively.

Now that we have estimates of the masses of the program stars' companions, their true nature can be constrained. The systems can be divided into three groups: 55 Cnc and 51 Peg with large metallicities, small eccentricities, small orbital radii, and companion masses near 1 M_J, 47 UMa with a smaller metallicity, a larger circular orbit, and a larger companion mass, and 70 Vir and HD 114762 with low metallicities, large eccentricities, moderate orbital radii, and much larger companion masses. It is likely that 70 Vir B and HD 114762 B are brown dwarfs or maybe even very low mass M dwarfs, but the uncertainties do not rule out the possibility that they are massive Jovian-type planets.

Of relevance to 51 Peg is the fact that tidally locked close binaries (orbital periods of a few days) have lithium abundances larger than their single star counterparts (Soderblom et al. 1990; Balachandran et al. 1993). If, contrary to our findings, the 51 Peg system has a very small orbital inclination and its companion is of stellar mass, then its lithium abundance would likely have been larger than we measured. Also, the rotation period of 51 Peg does not allow the possibility that this is a tidally locked system (Mayor & Queloz pointed out that the lack of synchronization on Gyr timescales is a strong argument against a stellar mass companion for 51 Peg).

4.3. Possible Source of High [Fe/H]

The high [Fe/H] values found for 51 Peg and 55 Cnc require explanation. It is too much to ascribe to coincidence the presence of two SMR stars in the small sample of planetary system candidates. It is also difficult to accept the possibility that 55 Cnc was born with its present photospheric composition given its great age and given the scarcity of old metal-rich stars in the Sun's vicinity. We propose instead that the original photospheric compositions of 55 Cnc and 51 Peg have been altered by the same processes that lead to the creation of the unusual planetary systems found around these stars. Our discussion will be limited to a comparison of 51 Peg to the Sun given their close similarities.

Lin et al. (1996) have proposed that 51 Peg B, if it is indeed a gas giant, was formed at about 5 AU from the star and at early times (within a few million years of its formation) migrated inward as a result of interactions with the circumstellar disk. The disk material (and presumably protoplanets) inside the orbit of 51 Peg B would have fallen into the star. Since much of this material would have been inside the so- called "ice-boundary", much of it would have consisted of refractory elements (essentially everything except H and He). This accreted material would have been mixed throughout the convective envelope of the parent star.

Using the present Solar System as a model, we can estimate the effect on the photospheric abundances of the Sun had it ingested Mercury, Venus, Earth, and Mars in its early history. Sackmann et al. (1993) calculate that at an age of about 30 Myrs the convective region of the Sun contained about 0.03 $M_{\odot}$. Assuming a composition similar to the C1 chondrites (Anders & Grevesse 1989), the addition of the terrestrial planets at this time would have dumped 2.18 x 10^{27} g of Fe into the convection zone, leading to an increase of [Fe/H] in the photosphere of 0.01 dex. The addition of 20 $M_{\oplus}$, which is still only 0.06 M_J, would have resulted in an increase of 0.11 dex, a detectable change. The timing of the

accretion is critical, as the stellar convection zone rapidly shrank in size during the first few million years of the Sun's existence; add the material too early, and it is diluted throughout a large volume. The timescale for the evolution of the protostellar disk is about 5 x 10^6 yr (Strom et al. 1993).

The next logical question to ask is, Why did the Solar System and the 51 Peg systems evolve differently? After all, both stars are of similar spectral types. The primary difference seems to be the composition of their photospheres. If 51 Peg was originally slightly more metal-rich than the Sun, then this would have resulted in the formation of a protoplanetary disk more abundant in refractory elements, which might have lead to the more rapid formation of protoplanets. A slightly more massive disk may have also lead to greater transfer of mass into the parent star (Laughlin & Bodenheimer 1994). Hence, according to this scenario, a more metal- rich star is more likely to alter its surface composition during the protostellar disk evolution phase than a similar but less metal-rich one. This is consistent with the similarity of the 47 UMa system to the Solar System. The companion of 47 UMa orbits at about 2 AU in a low eccentricity orbit (Butler & Marcy 1996), apparently having avoided the orbital decay phenomenon experienced by 51 Peg B. The metallicity of 47 UMa is also less than that of 51 Peg. Therefore, it appears from this small sample that the cutoff value of [Fe/H], below which the drag phenomenon will not operate efficiently, is between about +0.1 and +0.2 dex.

This hypothesis can be tested by comparing the compositions of planetary system candidates that are in wide-separation binaries. So far, 55 Cnc is the only such system; it is a common proper motion pair (Duquennoy & Mayor 1991). Unfortunately, its companion is an M5 dwarf with m_v = 13.2, which makes an accurate abundance analysis very difficult. A careful photometric analysis would probably be the best course of action at this time.

If the photospheres of 55 Cnc and 51 Peg are metal-rich relative to their interiors,

then evolutionary ages derived above are not correct. The metallicity affects not only the effective temperature and radius but also the luminosity. However, this may not fully account for the apparent great age of 55 Cnc. It was shown in §4.2, using other age indicators, that 55 Cnc is probably older than 51 Peg or 47 UMa.

5. Conclusions

We have undertaken spectroscopic abundance analyses of the five recently announced planetary system candidates. The metallicity is less than solar for HD 114762, approximately solar for 70 Vir and 47 UMa, and greater than solar for 55 Cnc and 51 Peg. We have also estimated the projected rotational velocities and employed them, along with other data, to estimate the most likely masses of the substellar companions of the program stars. The systems fall into three groups: 51 Peg B (mass $\approx$ 0.51 $M_{\rm J}$) and 55 Cnc B (mass ¿ 0.6 $M_{\rm J}$) - both SMR stars with small eccentricities and very small orbital distances, 47 UMa B at $\approx$ 4.6 $M_{\rm J}$ orbiting at about 2 AU, and 70 Vir B and HD 114762 B at ¿ 10 - 20 $M_{\rm J}$ with large eccentricities.

The most surprising, and potentially most important, findings in this study are the high metallicities of 55 Cnc and 51 Peg. These results are consistent with the planetary orbital migration model whereby a gas giant migrates to within a few hundredths of an AU of the parent star; the material between the planet and the star is presumably accreted onto the latter. If this is confirmed by future observations, then Galactic chemical evolution models will have to be revised accordingly. Also, we encourage researchers to direct their planetary search efforts at other SMR dwarfs and subgiants.

In order to improve the mass estimates of the companions, future research should be directed at refining the $v \sin i$ estimates through the use of very high resolution spectroscopy.

Improvements in the $M_{\rm V}$ estimates will occur when the HIPPARCOS dataset becomes available for the other planet candidates in the near future; this will lead to improved estimates of the stellar radii, masses, and ages. Additional theoretical work needs to be done on the planet migration process, the role of metallicity in the planet formation process, the early evolution of the depth of the convection zone in solar-type stars, and stellar models with metal-rich envelopes.

The author would like to especially thank David L. Lambert and Eric Bakker for obtaining high resolution spectra of the program stars at his request and for providing helpful suggestions. Additional helpful comments were given by Jocelyn Tomkin and Suchitra Balachandran. Thanks also go to Geoff Marcy for providing a list of his target stars and to Bengt Edvardsson for providing the EW measurements of 51 Peg used in the Edvardsson et al. (1993) paper. This research has made use of the Simbad database, operated at CDS, Strasbourg, France. The research has been supported in part by the National Science Foundation (Grant AST-9315124) and the Robert A. Welch Foundation of Houston, Texas.

Table 1. Atomic Data for Lines Used Here and not Listed by Gonzalez & Lambert (1996).

Spectral line	λ(Å)	χ_1(eV)	$EW_\odot$(mÅ)	$\log gf$
C I	6587.61	8.53	13.0	−1.20
O I	7771.94	9.14	70.6	0.25
O I	7774.16	9.14	62.7	0.13
O I	7775.38	9.14	48.4	−0.11
Na I	5688.20	2.10	121.4	−0.65
Al I	7835.29	4.02	45.0	−0.74
Al I	7836.11	4.02	58.6	−0.57
Si I	5793.06	4.93	44.3	−1.96
Ca I	5867.55	2.93	24.7	−1.62
Ca I	6455.59	2.52	57.3	−1.40
Cr I	5783.07	3.32	32.5	−0.45
Cr I	5783.87	3.32	44.7	−0.21
Fe I	6089.57	5.02	37.0	−0.91
Fe I	6093.65	4.61	31.0	−1.40
Fe I	7583.78	3.02	85.7	−1.95
Fe I	7586.01	4.31	135.3	−0.20
Fe I	7588.29	5.03	28.0	−1.14
Co I	6454.98	3.63	14.5	−0.32

Table 2. Atmospheric Parameters Derived from Fe-Line Analysis.

Star	T_{eff}(K)	$\log g$	ξ_t(km s^{-1})	[Fe/H]	N(Fe I,Fe II)
55 Cnc	5250 ± 100	4.30 ± 0.05	1.0 ± 0.20	0.24 ± 0.09	14, 6
51 Peg	5750 ± 100	4.40 ± 0.10	1.0 ± 0.10	0.22 ± 0.07	26, 5
47 UMa	6000 ± 100	4.55 ± 0.05	1.0 ± 0.10	0.10 ± 0.06	20, 5
70 Vir	5600 ± 100	4.10 ± 0.10	1.0 ± 0.10	0.04 ± 0.07	21, 4
HD 114762	6000 ± 100	4.50 ± 0.05	1.0 ± 0.10	-0.57 ± 0.06	17, 3

Table 3. Sensitivities of Calculated Abundances to Changes in Model Atmosphere Parameters for 51 Peg.

Line,λ(mÅ),EW(mÅ)	$\Delta T_{\rm eff}$ = +250 K	$\Delta \log g$ = +0.5 (cgs)	$\Delta\xi_{\rm t}$ = +0.5 km s^{-1}	ΔEW= +2%
O I, 7774.16, 75	−0.24	+0.10	−0.05	+0.10
Ca I, 6455.59, 70	+0.18	−0.07	−0.10	+0.11
Sc II, 6604.58, 50	−0.01	+0.21	−0.10	+0.09
Fe I, 6750.15, 87	+0.21	−0.06	−0.20	+0.16
Fe I, 7588.29, 39	+0.10	−0.02	−0.05	+0.07
Fe II, 6432.68, 47	−0.11	+0.22	−0.10	+0.11

Table 5. Values of T_{eff} for Program Stars from other Sources.

Star	β	$b-y$	T_{eff}(Ed. et al.)[a]	$T_{eff}(b-y)$[a]	$T_{eff}(\beta)$[a]	$<T_{eff}>$[b]	$\log g$[c]	[Fe/H][c]
51 Peg	2.603	0.416	5755	5725	5889	5779	4.44	0.24
47 UMa	2.606	0.392	5882	5850	5923	5943	4.45	0.09
70 Vir	2.576	0.446	...	5522	5578	5575	4.05	0.03
HD 114762	2.590	0.363	5871	5887	5742	5907	4.39	−0.61

[a]$T_{eff}(b-y)$ and T_{eff} were estimated from the Strömgren photometry given by Hauck & Mermilliod (1980) and using Equation 1. Ed. et al. refers to Edvardsson et al. (1993).

[b]The mean value of T_{eff} was calculated from the two photometric estimates, with half weight given to each, and the spectroscopic estimates of this study.

[c]These new $\log g$ and [Fe/H] estimates are based on $<T_{eff}>$.

Table 6. Final Adopted Abundances for the Program Stars.

Element	$\log \epsilon_{\odot}$	55 Cnc [X/H]	N	51 Peg [X/H]	N	47 UMa [X/H]	N	70 Vir [X/H]	N	HD 114762 [X/H]	N
Li	1.06	<0.56	1	1.50±0.11	1	1.90±0.07	1	1.85±0.07	1	2.77±0.07	1
C	8.55	0.22±0.15	1	0.12±0.12	2	−0.05±0.12	2	−0.05±0.12	2	−0.54±0.11	1
O	8.94	···	···	0.24±0.11	3	0.10±0.11	3	−0.07±0.11	3	···	···
Na	6.34	0.33±0.13	2	0.18±0.09	3	0.20±0.09	1	0.04±0.10	1	−0.40±0.09	1
Mg	7.61	···	···	0.15±0.11	1	0.04±0.09	1	−0.01±0.11	1	−0.38±0.09	1
Al	6.51	0.52±0.12	1	0.29±0.08	3	0.01±0.07	2	0.11±0.09	2	···	···
Si	7.58	0.39±0.14	1	0.21±0.11	3	0.08±0.07	2	−0.01±0.08	2	−0.41±0.07	2
S	7.29	···	···	0.22±0.13	1	0.09±0.11	1	···	···	···	···
Ca	6.37	0.30±0.10	2	0.16±0.09	3	0.13±0.08	2	0.03±0.08	3	−0.44±0.09	1
Sc	3.11	···	···	0.33±0.07	2	0.18±0.05	2	0.13±0.07	2	−0.45±0.05	2
Ti	4.96	0.25±0.09	2	0.24±0.07	4	0.21±0.06	2	0.12±0.08	4	−0.28±0.05	4
Cr	5.71	0.34±0.09	2	0.25±0.08	2	0.12±0.07	2	0.07±0.08	2	−0.70±0.08	1
Fe	7.53	0.24±0.09	20	0.22±0.07	31	0.10±0.06	25	0.04±0.07	25	−0.57±0.06	20
Co	4.93	0.49±0.11	1	0.30±0.08	2	···	···	0.00±0.09	1	···	···
Ni	6.27	0.29±0.16	1	0.31±0.08	2	0.15±0.07	1	0.03±0.09	1	−0.51±0.06	2
Y	2.25	···	···	···	···	0.04±0.07	1	−0.12±0.09	1	−0.66±0.06	2
Ba	2.23	0.14±0.12	1	0.17±0.10	1	0.20±0.07	1	−0.02±0.09	1	−0.76±0.07	1

Note. — The uncertainties in [X/H] are a combination of the random and systematic (uncertainties in atmospheric parameters) error sources. The lithium abundances are given as $\log \epsilon$, rather than [X/H].

Table 7. Measured Values of Macroturbulent and Rotational Line Broadening.

Star Fe I line	$\zeta_{\rm RT}$ km s^{-1}	$v \sin i$ km s^{-1}
Sun		
5379.586	3.55±0.05	≡1.9
5638.249	3.55±0.05	≡1.9
5379.586	3.60±0.10	1.9±0.1
5638.249	3.50±0.10	2.0±0.1
55 Cnc		
5379.586	2.7±0.3	1.2±0.7
5638.249	2.2±0.4	1.9±0.7
51 Peg		
6213.435	3.50±0.30	2.0±0.5
6322.691	4.10±0.30	1.5±0.7
47 UMa		
5379.586	4.10±0.20	1.9±0.6
5638.249	3.95±0.20	1.9±0.7
70 Vir		
5379.586	4.05±0.05	0.4±0.4
5638.249	4.10±0.10	0.5±0.5
HD 114762		
5379.586	4.1±0.1	1.0±1.0
5638.249	4.1±0.1	1.0±0.6

Table 8. Age and Mass Estimates of Program Stars Using VandenBerg Evolutionary Tracks.

Star	$M_{\rm V}$ (phot.)	$M_{\rm V}$ (astrom.)	$M_{\rm V}$ (adopted)	Age (Gyr) ($\rm M_v - T_{eff}$)	Mass ($\rm M_{\odot}$)	Age (Gyr) (Ed. et al.)
55 Cnc	···	$5.28^{+0.08}_{-0.07}$	5.28±0.08	13±2	0.90±0.02	···
51 Peg	3.7±0.2	4.56±0.04	4.56±0.04	3^{+2}_{-1}	1.13±0.03	8.5
47 UMa	4.1±0.2	4.31±0.03	4.31±0.03	5±1	1.10±0.02	6.9
70 Vir	3.7±0.2	3.71±0.04	3.71±0.04	7.0±0.5	1.20±0.01	···
HD 114762	4.6±0.2	···	4.6±0.20	17±3	0.79±0.02	13.8

REFERENCES

Anders, E. & Grevesse, N. 1989, Geochim. Cosmochim. Acta, 53, 197

Balachandran, S., Carney, B. W., Fry, A. M., Fullton, L. K., & Peterson, R. C. 1993, ApJ, 413, 68

Baliunas, S., Sokoloff, D., & Soon, W. 1996, ApJ, 457, L99

Baranne, A., Mayor, M., & Poncet, J. L. 1979, Vistas Astr., 23, 279

Butler, R. P. & Marcy, G. W. 1996, ApJ, 464, 153

Campbell, B., Walker, G. A. H., & Yang, S. 1988, ApJ, 331, 902

Cayrel de Strobel, G., Hauck, B., Francois, P., Thevenin, F., Friel, E., Mermilliod, M., & Borde, S. 1992, A&AS, 95, 273

Cochran, W. D., Hatzes, A. P., & Hancock, T. J. 1991, ApJ, 380, L35

Cochran, W. D., & Hatzes, A. P. 1994, in "Planetary systems: Formation, Evolution, and Detection," (Kluwer Academic, B. Burke, J. H. Rahe, & E. E. Roettger, eds.), 281

Cunha, K., Smith, V. V., & Lambert D. L. 1995, ApJ, 452, 634

Dorren, J. D., Guinan, E. F., & Dewarf, L. E. 1994, in "Cool Stars, Stellar Systems, and the Sun," (Astronomical Society of the Pacific, J. Caillault, ed.), 399

Dravins, D., Lindegren, L., Nordlund, A., & VandenBerg, D. A. 1993, ApJ, 403, 385

Duquennoy, A. & Mayor, M. 1991, A&A, 248, 485

Durrant, C. J. 1979, A&A, 76, 208

Edvardsson, B., Anderson, J., Gustafsson, B., Lambert, D. L., Nissen, P. E., & Tomkin, J. 1993, A&A, 275, 101

Eggen, O. J. 1969, PASP, 81, 553

Favata, F., Micela, G., & Sciortino, S. 1996, A&A, preprint

François, P., Spite, M., Gillet, D., Gonzalez, J.-F., & Spite, F. 1996, A&A, 310, L13

Gonzalez, G. & Lambert, D. L. 1996, AJ, 111, 424

Guinan, E. 1995, IAU Circ.6261

Gray, D. F. 1977, ApJ, 218, 530

Gray, D. F. 1984, ApJ, 281, 719

Gray, D. F. 1992, The Observation and Analysis of Stellar Photospheres (Cambridge: Cambridge University Press)

Hauck, B. & Mermilliod, M. 1990, A&AS, 86, 107

Kurucz, R. L., Furenlid, I., Brault, J., & Testerman, L. 1984, Solar Flux Atlas from 296 to 1300 nm (Sunspot, NM: National Solar Observatory)

Kurucz, R. 1992, ATLAS9 Stellar Atmosphere Programs and 2km/s Grid CDROM Vol. 13 (Cambridge: Smithsonian Astrophysical Observatory)

Lambert, D. L., Heath, J. E., & Edvardsson, B. 1991, MNRAS, 253, 610

Latham, D. W., Mazeh, T., Stefanik, R. P., Mayor, M., & Burki, G. 1989, Nature, 339, 38

Laughlin, G. & Bodenheimer, P. 1994, ApJ, 436, 335

Lin, D. N. C., Bodenheimer, P., & Richardson, D. C. 1996, Nature, 380, 606

Lutz, T. E. & Kelker, D. H. 1973, PASP, 85, 573

Marcy, G. W. & Butler, R. P. 1996a, ApJ, 464, 147

Marcy, G. W. & Butler, R. P. 1996b, World Wide Web site at http://cannon.sfsu.edu∼williams/planetsearch/planetsearch.html

Marsakov, V. A. & Shevelev, Yu. G. 1995, BICDS, 47, 13

Mayor, M. & Queloz, D. 1995, Nature, 378, 355

McCarthy, J. K., Sandiford, B. A., Boyd, D., & Booth, J. 1993, PASP, 105, 881

Nissen, P. E. 1988, A&A, 199, 146

Nissen, P. E. 1994, Rev. Mexicana Astron. Astrofis., 29, 129

Rocha-Pinto, H. J. & Maciel, W. J. 1996, MNRAS, 279, 447

Sackmann, I.-J., Boothroyd, A. I., & Kraemer, K. E. 1993, ApJ, 418, 457

Soderblom, D. R. 1982, ApJ, 263, 239

Soderblom, D. R. 1983, ApJS, 53, 1

Soderblom, D. R. 1985, AJ, 90, 2103

Soderblom, D. R., Oey, M. S., Johnson, D. R. H., & Stone, R. P. S. 1990, AJ, 99, 595

Strom, S. E., Edwards, S., & Skrutskie, M. F. 1993, in Protostars and Planets III, ed. E. Levy & J. Lunine (Tucson: Univ. Arizona Press), 837

Takeda, Y. 1995, PASJ, 47, 337

Takeda, Y., Kato, K., Watanabe, Y., & Sadakane, K. 1996, PASJ, 48, 511

Taylor, B. J. 1996, ApJS, 102, 105

Tull, R. G., MacQueen, P. J., Sneden, C., & Lambert, D. L. 1995, PASP, 107, 251

van Altena, W. F., Lee, J. T., & Hoffleit, D. 1995, The General Catalogue of Trigonometric Stellar Parallaxes, Fourth Edition (New Haven: Yale University Observatory)

VandenBerg, D. A. 1985, ApJS, 58, 711

Walker, G. A. H., Walker, A. R., Irwin, A. W., Larson, A. M., Yang, S. L. S., & Richardson, D. C. 1995, Icarus, 116, 359

This manuscript was prepared with the AAS LaTeX macros v4.0.

Fig. 1.— Portions of the spectra of 51 Peg and the Sun (reflected off the asteroid Vesta) containing the Li I line and two Fe I lines of moderate strength. The spectra were obtained with the same instrument (on different dates); the resolutions have been matched by smoothing the (slightly) higher resolution spectrum. The Sun and 51 Peg have nearly identical physical parameters; hence, the stronger lines in the spectrum of 51 Peg are due to a greater Fe abundance.

Fig. 2.— The Fe I (filled circles) and Fe II (plus signs) abundances calculated using the model parameters given in Table 2 are plotted versus the lower excitation potential ($\chi_{\rm l}$) and $\log{(EW/\lambda)}$. The solid lines are least-squares fits through the Fe I data points. The dotted lines in the first diagram are the least-squares fits when $T_{\rm eff}$ is changed by $\pm$ 250 K. The dotted lines in the second diagram are the least-squares fits when $\xi_{\rm t}$ is changed by $\pm$ 0.2 km s^{-1}. Even though the lower dotted line in the second diagram (corresponding to $\xi_{\rm t}$ = 1.2 km s^{-1}) appears to be a better solution, it was not chosen because the slopes of the least-squares fits have been affected by the two strong Fe I lines near $\log{(EW/\lambda)}$ = -4.7. These two points do not affect the $T_{\rm eff}$ estimate significantly since they have very different values of $\chi_{\rm l}$.

Fig. 3.— Best-fit synthetic profile (solid curve) of the Fe I line at 5638.28 Å in the spectrum of 70 Vir using $\zeta_{\rm RT}$ = 4.1 and $v \sin i$ = 0.5 km s^{-1}; the dotted curve corresponds to $\zeta_{\rm RT}$ = 4.2 and $v \sin i$ = 0.0 km s^{-1} and the dashed curve to $\zeta_{\rm RT}$ = 3.8 and $v \sin i$ = 1.4 km s^{-1}. Also shown are the residual differences between the observations and the synthesis; the large low frequency fluctuations in this plot are due to a slight asymmetry in the observed line profile. Although all three residual plots appear very similar to visual inspection, the best fit was chosen in a quatitative manner as the one with the smallest standard deviation.

Fig. 4.— Histogram of the distribution of photometric [Fe/H] estimates for F5 to G2 dwarfs within 80 pc of the Sun determined by Marsakov & Shevelev (1995). The average [Fe/H]

value is indicated by a solid line and the program stars by dotted lines. The [Fe/H] values of the program stars are from this study.

TABLE 4

Estimated Abundances for Individual Spectral Lines

Element, ($\log \epsilon_{\odot}$) Wavelength(Å)	55 Cnc EW,[X/H],[X/Fe]	51 Peg EW,[X/H],[X/Fe]	47 UMa EW,[X/H],[X/Fe]	70 Vir EW,[X/H],[X/Fe]	HD 114762 EW,[X/H],[X/Fe]
Li I, (1.06)*					
6707.8	SS,< −0.50,< −0.74	SS,0.44,0.24	SS,0.84,0.74	SS,0.79,0.75	SS,1.71,2.28
C I, (8.55)					
5380.31	21,0.22,−0.02	28,0.10,−0.12	24,−0.10,−0.19	22,−0.08,−0.12	10,−0.54,0.03
6587.62	···	17,0.13,−0.09	17,0.01,−0.09	13,−0.01,−0.05	···
O I, (8.94)					
7771.94	···	89,0.26,0.04	89,0.05,−0.05	61,−0.08,−0.12	···
7774.16	···	75,0.21,−0.01	83,0.09,−0.01	53,−0.11,−0.15	···
7775.38	···	64,0.26,0.04	71,0.16,0.06	45,−0.02,−0.06	···
Na I, (6.34)					
5688.20	···	150,0.27,0.05	129,0.20,0.10	122,0.04,0.00	72,−0.40,0.17
6154.23	98,0.37,0.13	57,0.18,−0.04	···	···	···
6160.75	117,0.28,0.04	71,0.08,−0.14	···	···	···
Mg I, (7.61)					
5711.08	···	125,0.15,−0.07	107,0.04,−0.06	112,−0.01,−0.05	75,−0.38,0.19
Al I, (6.51)					
6698.65	67,0.52,0.28	36,0.30,0.08	···	···	···
7835.29	···	68,0.29,0.07	39,−0.01,−0.11	58,0.15,0.11	···
7836.11	···	84,0.29,0.07	54,0.02,−0.08	65,0.07,0.03	···
Si I, (7.58)					
5793.06	69,0.39,0.15	57,0.23,0.01	46,0.10,0.00	50,0.05,0.01	22,−0.37,0.20
5948.54	···	102,0.13,−0.09	···	···	···
6721.85	···	67,0.27,0.05	49,0.06,−0.04	44,−0.07,−0.11	21,−0.45,0.12
S I, (7.29)					
6052.65	···	18,0.22,0.00	17,0.09,−0.01	···	···
Ca I, (6.37)					
5867.55	59,0.31,0.07	32,0.15,−0.07	24,0.11,0.01	26,−0.05,−0.09	···
6455.59	99,0.29,0.05	70,0.20,−0.02	···	62,−0.01,−0.05	26,−0.44,0.13
6471.65	···	102,0.13,−0.08	94,0.14,0.04	104,0.14,0.10	···
Sc II, (3.11)					
5526.80	···	91,0.33,0.11	86,0.19,0.09	89,0.15,0.11	61,−0.44,0.13
6604.58	···	50,0.33,0.11	42,0.17,0.07	48,0.11,0.07	20,−0.46,0.11
Ti I, (4.96)					
6126.21	71,0.36,0.12	36,0.27,0.05	23,0.23,0.13	35,0.10,0.06	8,−0.30,0.27
6261.09	···	63,0.27,0.05	48,0.20,0.10	63,0.12,0.08	24,−0.27,0.30
Ti II, (4.96)					
5336.78	···	80,0.23,0.01	···	83,0.17,0.13	66,−0.21,0.36
5418.77	55,0.14,−0.10	57,0.18,−0.04	···	60,0.10,0.06	63,−0.35,0.22
Cr I, (5.71)					
5783.07	67,0.28,0.04	43,0.20,−0.02	31,0.11,0.01	39,0.04,0.00	···
5783.87	89,0.41,0.17	61,0.29,0.07	44,0.13,0.03	54,0.10,0.06	11,−0.70,−0.13
Fe I, (7.53)					
5044.21	···	89,0.42,—	···	82,0.19,—	37,−0.50,—
5288.52	···	71,0.16,—	59,0.05,—	63,−0.07,—	27,−0.60,—
5322.04	···	73,0.20,—	63,0.16,—	70,0.01,—	24,−0.66,—
5554.90	···	119,0.41,—	···	100,0.18,—	46,−0.58,—
5560.21	76,0.16,—	63,0.17,—	52,0.08,—	58,0.02,—	20,−0.60,—
5576.09	···	145,0.30,—	120,0.16,—	127,0.10,—	74,−0.55,—

TABLE 4—*Continued*

Element, ($\log \epsilon_{\odot}$) Wavelength(Å)	55 Cnc EW,[X/H],[X/Fe]	51 Peg EW,[X/H],[X/Fe]	47 UMa EW,[X/H],[X/Fe]	70 Vir EW,[X/H],[X/Fe]	HD 114762 EW,[X/H],[X/Fe]
5859.57	107,0.29,—	86,0.24,—	76,0.18,—	77,0.07,—	34,−0.56,—
5862.35	130,0.26,—	108,0.26,—	87,0.07,—	89,0.00,—	48,−0.58,—
6024.06	···	135,0.23,—	110,0.06,—	119,0.09,—	66,−0.57,—
6027.05	88,0.06,—	76,0.12,—	64,0.02,—	71,−0.03,—	28,−0.68,—
6065.48	···	139,0.21,—	119,0.11,—	129,0.04,—	80,−0.51,—
6089.56	63,0.28,—	···	···	···	···
6093.63	54,0.24,—	···	···	···	···
6165.36	69,0.18,—	56,0.18,—	···	···	···
6213.43	122,0.16,—	···	···	···	···
6232.63	···	104,0.32,—	···	···	···
6252.57	···	134,0.13,—	···	129,0.02,—	75,−0.62,—
6265.14	···	98,0.21,—	86,0.15,—	95,0.04,—	···
6335.34	···	108,0.13,—	97,0.11,—	116,0.18,—	63,−0.50,—
6430.85	···	126,0.10,—	111,0.04,—	122,−0.03,—	75,−0.55,—
6593.87	128,0.33,—	99,0.29,—	83,0.16,—	92,0.06,—	45,−0.54,—
6703.55	65,0.18,—	49,0.22,—	34,0.11,—	50,0.11,—	9,−0.63,—
6750.15	112,0.27,—	87,0.24,—	73,0.14,—	82,0.04,—	···
6752.70	···	49,0.21,—	34,0.04,—	···	14,−0.47,—
6806.84	70,0.32,—	···	···	···	···
6810.26	81,0.30,—	65,0.25,—	···	···	···
6820.36	75,0.42,—	53,0.25,—	41,0.14,—	···	···
7583.78	···	96,0.16,—	82,0.07,—	95,0.06,—	···
7586.01	···	147,0.16,—	128,0.07,—	123,−0.08,—	···
7588.29	···	39,0.22,—	27,0.08,—	33,0.05,—	···
Fe II, (7.53)					
5234.62	78,0.05,—	97,0.24,—	88,−0.03,—	83,−0.10,—	67,−0.57,—
5414.08	34,0.42,—	40,0.37,—	31,0.08,—	34,0.13,—	13,−0.55,—
6084.10	19,0.16,—	27,0.19,—	25,0.08,—	27,0.06,—	···
6149.25	35,0.25,—	···	···	···	···
6369.45	···	24,0.19,—	23,0.12,—	···	···
6247.56	49,0.24,—	···	···	nodata	···
6432.68	43,0.28,—	47,0.14,—	46,0.03,—	49,0.06,—	23,−0.62,—
Co I, (4.93)					
6454.98	43,0.29,0.25	25,0.32,0.10	···	18,0.00,−0.04	···
6814.96	···	30,0.27,0.05	···	···	···
Ni I, (6.27)					
5082.34	···	82,0.39,0.17	···	···	30,−0.54,0.03
6767.76	115,0.29,0.05	92,0.23,0.01	80,0.15,0.05	88,0.03,−0.01	46,−0.49,0.08
Y II, (2.25)					
4883.69	···	···	···	···	41,−0.56,0.01
5087.42	···	···	52,0.04,−0.16	52,−0.12,−0.16	25,−0.75,−0.18
Ba II, (2.23)					
5853.67	75,0.14,−0.10	71,0.17,−0.05	73,0.20,0.10	70,−0.02,−0.06	39,−0.76,−0.19

Note.—The lithium abundance was estimated using spectrum synthesis as described in the text. The quoted solar lithium abundance is that of the photosphere. The othe solar abundances are meteoritic estimates from Gonzalez & Lambert (1996).